CO IN NEARBY NORMAL GALAXIES

YOSHIAKI SOFUE
Institute of Astronomy, University of Tokyo, Mitaka, Tokyo 181, Japan

Abstract. We review CO line observations of nearby galaxies, particularly those with high-resolution and high-sensitivity using large aperture telescopes such as the Nobeyama 45 m and and IRAM 30 m telescopes. Based on the observations, we discuss kinematics of the molecular gas, including the inner rotation curves of galaxies, and interstellar physics including the galactic scale HI–molecule transition and the CO to H_2 conversion factor.

1. Introduction

CO observations of galaxies provide information about: (A) Distribution and approximate mass of molecular hydrogen gas. Face-on galaxies show us the radial distribution and spiral arm related density enhancements. High-resolution mapping of edge-on galaxies tells us about the vertical extent of the molecular disk and halo. Accurate information on gas masses cannot be obtained as yet because of the uncertainty in the CO-to-H_2 conversion factor. (B) Kinematics of the molecular gas, particularly in the inner region of galaxies, thanks to the high velocity resolutions. This provides detailed rotation curves for the inner 1 kpc, kinematics of non-circular motions related to bar-shocked gas, which is related to triggering enhanced star formation in the nuclei, and density wave kinematics in the disk. And (C) Physical properties of the interstellar molecular gas, such as the temperature, density, or clumpiness from multi-transition observations.

The major constituents of interstellar matter (ISM) in spiral galaxies are HI and H_2 gas, which share several to ten percent of the total mass. HI gas distributions have been determined for many galaxies from high-resolution maps. It is, however, only recently that a number of galaxies have been mapped in the CO line with high resolution and sufficient sensitivity by using large filled aperture dishes like the Nobeyama 45 m and

W.B. Latter et al. (eds.), CO: Twenty-Five Years of Millimeter-Wave Spectroscopy, 273–281.

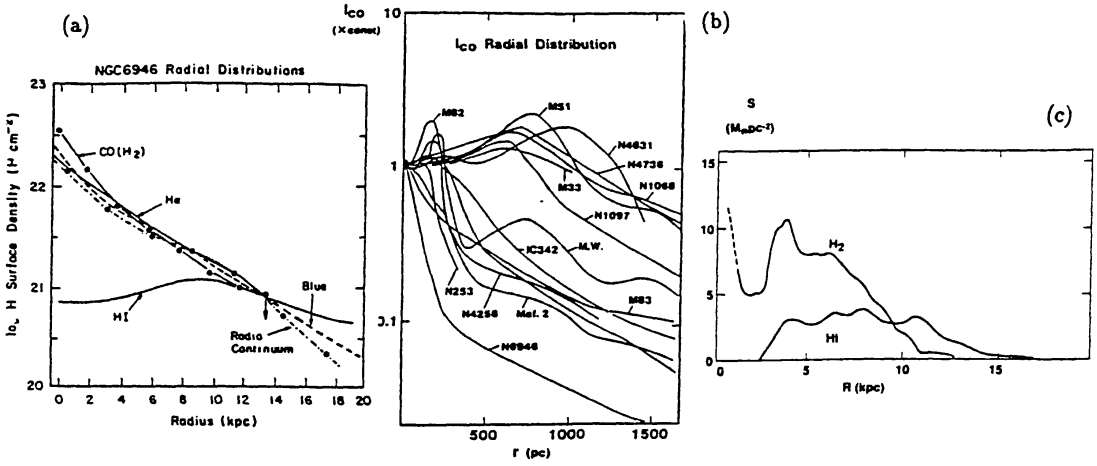

Figure 1. (a) I_{CO} distribution in the Sc galaxy NGC 6946. (b) I_{CO} distributions in the central regions of disk galaxies. (c) Radial distribution of I_{CO} in the Sb galaxy NGC 891.

IRAM 30 m telescopes. In this review we concentrate on results from large filled aperture telescopes and on nearby, well studied normal Sb and Sc spirals. Interferometric observations are reviewed by Scoville in this volume. Readers may also refer to reviews on CO in galaxies by Morris & Rickard (1982); Young & Scoville (1991); Combes (1991); and Sargent & Welch (1993).

2. Molecular Gas Distribution

2.1. RADIAL DISTRIBUTION

The global distribution of the CO line intensity indicates the molecular disks of late type (Sc, Sd) spiral galaxies are characterized as exponential disks with nuclear concentrations and superposed spiral arms. The central region often shows strong non-circular motions caused by a bar induced shock wave and inflow. In addition to these features, Sb and Sa galaxies usually show a large scale ring structure with a radius of a few kpc, similar to the 4 kpc molecular ring in the Milky Way. Fig 1. shows the I_{CO} distribution in the Sc galaxy NGC 6946, indicating an exponential disk (Young & Scoville 1982, 1991). The central region of this galaxy also has a steeper-exponential, high density disk (Fig. 1b) (Sofue 1990). The central regions of other galaxies generally exhibit more ring-like structures with radii of several hundred pc (Fig. 1b). The radial I_{CO} distribution in the Sb galaxy NGC 891 (Fig. 1c) shows a several-kpc molecular ring (Sofue & Nakai 1993).

In higher resolution CO maps, spiral arms show up in positional coincidence with the optical dark lanes inside the spiral arms. Optical arms,

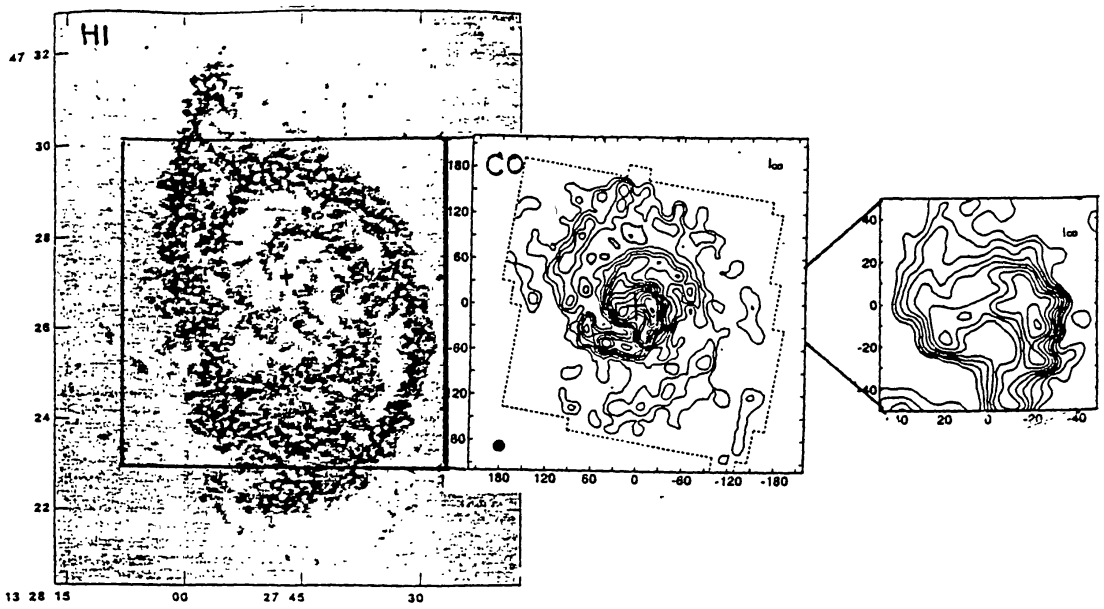

Figure 2. CO intensity distribution in the face-on galaxy M51 (Nakai et al. 1994) compared with a high-resolution HI map (Rots 1990).

particularly those seen in Hα emission and indicating massive star forming regions, are shifted slightly downstream from the CO spiral arms by 0.5–1 kpc in the azimuthal direction ($\sim$ 100 pc perpendicular to the arms) due to the time lag of $\sim 10^7$ yrs between the galactic shock compression of gas and star formation. Fig. 2 shows the CO intensity distribution in the face-on galaxy M51 observed with the Nobeyama 45 m telescope (Nakai et al. 1994) in comparison with a high-resolution HI VLA map (Rots et al. 1990). It is clear in this figure that the molecular gas dominates in the inner 3 kpc region, while HI dominates in the outer disk.

2.2. VERTICAL DISTRIBUTION

High resolution CO images of edge-on galaxies are useful for investigating the vertical extent of the molecular gas disk and halo. Fig. 3 shows the variation of the CO intensity perpendicular to the disk plane in the edge-on galaxy NGC 891 (Garcia-Burillo et al. 1992; Sofue & Nakai 1993). The molecular disk is unresolved, but a deconvolution of the profile using an assumed beam indicates the molecular disk is about 100 pc thick. Further data indicate the thickness increases with the distance from the center. In addition to this thin and dense disk, a thick halo component is detected, extending about ± 1 kpc above the galactic plane. The amount of molecular gas in this extended component amounts to a few tens of percent of the total CO emission, indicating a significant molecular gas in the halo.

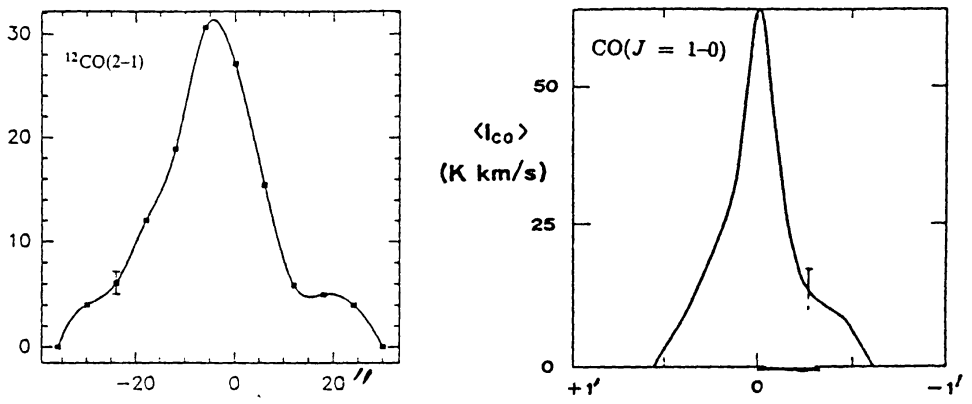

Figure 3. Variation of the CO intensity perpendicular to the disk plane in the edge-on galaxy NGC 891 (Garcia-Burillo et al. 1992; Sofue & Nakai 1993)..

3. Kinematics and Rotation

3.1. INNER CO + OUTER HI ROTATION CURVES

The rotation curves of galaxies have been obtained from optical and HI 21 cm line emission observations along the major axes (e.g., Rubin et al. 1982). Optical measurements are affected by the contamination of the bright bulge light, which increases the uncertainty of the curve near the center. The HI gas distribution has a depression in the central few kpc region, which yields an apparently solid rotation curve for the central few kpc. The CO-line emission on the other hand is concentrated in the central region, so it gives the most accurate rotation curves of the inner few kpc region.

A rotation curve can be derived by using the loci of terminal velocities in a PV diagram. Therefore, the velocity dispersion of the interstellar gas and the velocity resolution of observations must be corrected properly. Fig. 4a shows an example of a composite PV diagram for NGC 891 using CO data from Sofue & Nakai (1993) and HI data from Rupen (1991). The HI gas traces the rotation of the outer disk, whereas the CO emission traces the rotation in the innermost region including the rapidly rotating nuclear disk (see also Garcia-Burillo et al. 1992; Scoville et al. 1993). In Fig. 4b, we present rotation curves obtained this way for several galaxies (Sofue 1996). Generally, the rotation velocity rises steeply within a few hundred pc, indicating the existence of a central compact mass component. Many galaxies (the Milky Way, NGC 891, NGC 3079, NGC 6946) exhibit a sharp maximum at $R \sim$ a few hundred pc, reaching a velocity as high as $\sim$ 200 to 300 km s^{-1}.

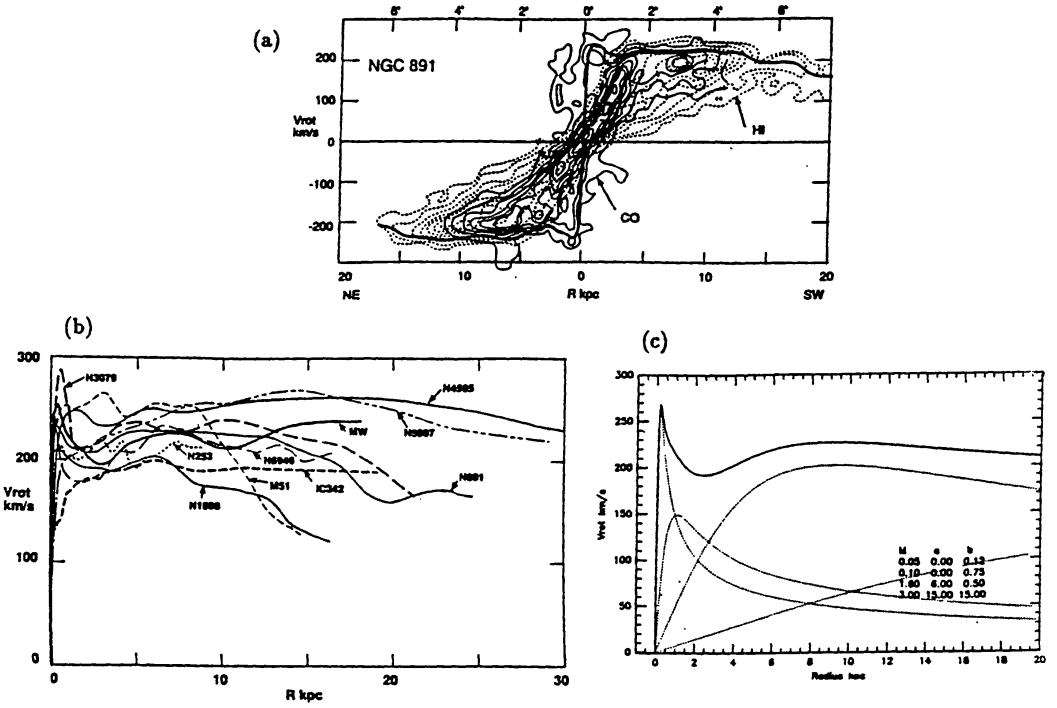

Figure 4. (a) CO + HI position-velocity diagram for NGC 891. (b) Most completely sampled rotation curves of galaxies. (c) A calculated rotation curve for a four-component model.

3.2. FITTING BY A POTENTIAL WITH FOUR MASS COMPONENTS

The observed rotation curves can be fitted by the Miyamoto-Nagai (MN) (1975) potential with multiple mass components. The rotation velocity is calculated from $V_{\rm rot} = (R\partial\Phi/\partial R)^{1/2}$, where Φ is the MN potential. The usual three-component model (bulge, disk, and halo) is not sufficient to fit the steep central peak, so we have to introduce a fourth, compact nuclear component. Fig. 4c shows an example of a calculated rotation curve of this four-component model ($n = 4$), where we assumed (1) nuclear compact mass, (2) bulge, (3) disk, and (4) massive halo components. This nuclear mass component has significant implications for the formation and evolution of the galactic bulge and the central mass condensation in galaxies.

3.3. VELOCITY FIELDS: NON-CIRCULAR MOTIONS

A velocity field, defined as the distribution of the intensity weighted mean velocity over a galaxy, provides information not only about rotation, but also about non-circular motions. Non-circular motions can arise from density waves, galactic shocks, bar-induced shocks, and inflows. The CO VF is useful to trace these effects in the central region of a galaxy, while the HI

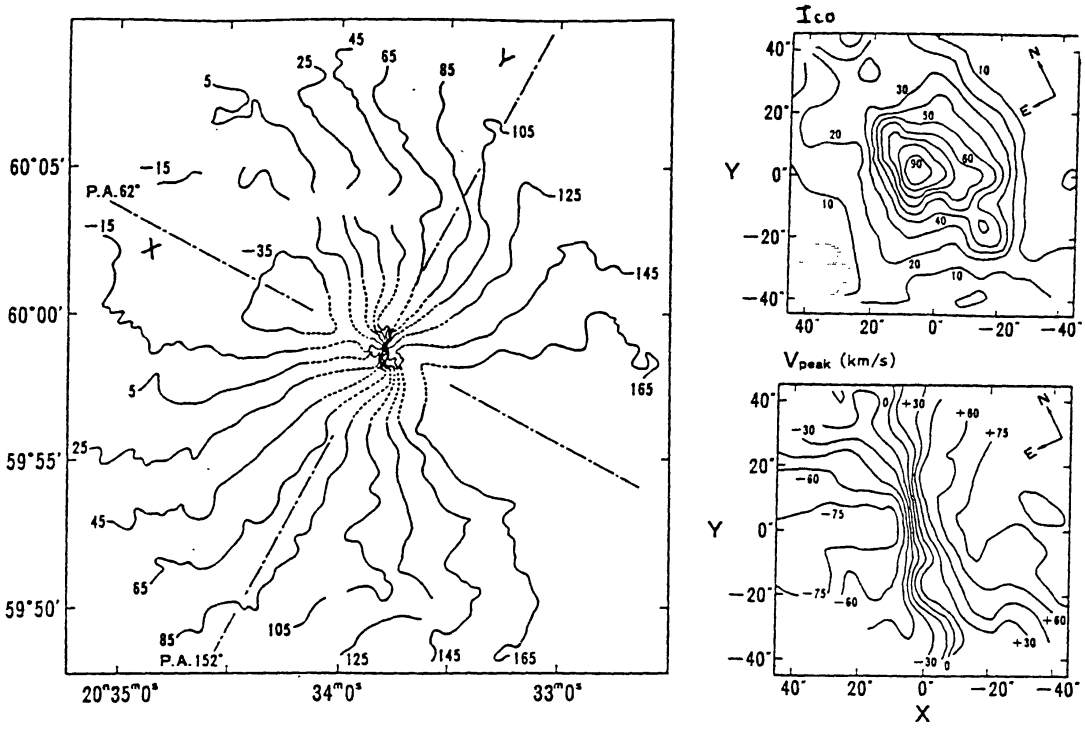

Figure 5. HI + CO velocity field for NGC 6946.

VF can be used to study the motion of the outer disk and outskirts (Bosma 1981). Fig. 5 shows an HI + CO velocity field for the face-on galaxy NGC 6946 (Sofue et al. 1988). Spiral arms show up by tracing loci with corrugated isovelocity contours, indicating velocities distorted from the circular motion

by a few to ten percent of the rotation ($\sim 10 - 30$ km s^{-1}). In M51, however, a larger non-circular motion has been detected in the spiral arms, exceeding 50 km s^{-1} (Garcia-Burillo et al. 1993). This is too large for a density wave and poses a crucial problem for arm formation theory. In general, the inner regions show larger non-circular motions, amounting to a few tens of percent of the rotation velocity ($\sim 30 - 50$ km s^{-1}) and much larger non-circular distortions are observed in the nuclear disks with interferometric measurements (e.g., Ishizuki et al. 1990). Such highly distorted velocity fields have been simulated extensively and suggest existence of a nuclear bar potential (e.g., Wada & Habe 1996 and the literature therein).

4. Physics of ISM in Galaxies

4.1. GALACTIC SCALE HI–H_2 TRANSITION: MOLECULAR FRONT

The HI and the gas density distributions derived from the HI and CO line intensities can be used to obtain distribution of the molecular fraction, de-

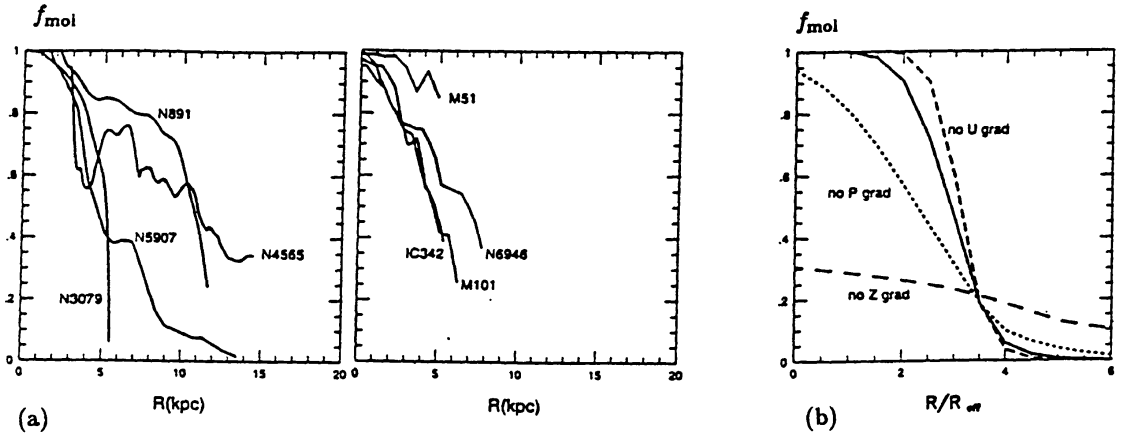

Figure 6. (a) Distributions of $f_{\rm mol}$ for several galaxies. (b) Model molecular front.

fined as $f_{\rm mol} = \rho_{\rm H_2}/(\rho_{\rm HI} + \rho_{\rm H_2})$. Fig. 6 shows the derived $f_{\rm mol}$ distributions for several galaxies (Sofue et al. 1994; Honma et al. 1995). The figure shows the ISM in the central few kpc is almost totally molecular, while the ISM is almost totally HI in the outer disk. The HI to H_2 transition occurs suddenly in a narrow range of radius, which we call the *molecular front.* The HI and H_2 disks are clearly separated by this front. The front will be the place where the phase transition from HI to H_2, and vice versa, is taking place on a galactic scale.

The observations can be well explained by a phase-transition theory proposed by Elmegreen (1993). The critical parameters for determining the molecular fraction $f_{\rm mol}$ are the interstellar pressure P, the UV radiation field U, and the metallicity Z. We constructed a model galaxy in which P, U, and Z are exponentially distributed with the radius r, $\propto \exp - r/r_e$, where r_e is the disk scale radius. Fig. 6b plots the calculated results, which indicate the molecular front is a fundamental feature of an exponential disk galaxy. Results for constant P and Z are also shown by dashed and dotted lines, but cannot reproduce the observations. The molecular front will have an important effect on the evolution of the interstellar matter in galaxies, which should be deeply coupled with the chemical evolution of galaxies from their birth.

4.2. THE CO-TO-H_2 CONVERSION FACTOR AND METAL ABUNDANCE

The mass of molecular gas has been derived from the CO intensity. This is, however, still very crude because of uncertainty in the conversion factor. The column density of H_2 molecules is assumed proportional to the integrated intensity of the ^{12}CO ($J = 1-0$) line, $N(\rm H_2)$ [cm^{-2}] $= X \int_{V_{\rm min}}^{V_{\rm max}} T_{\rm B} dv$ [K km s^{-1}]. Here $X = X^* \times 10^{20}$ is the conversion factor, for which we of-

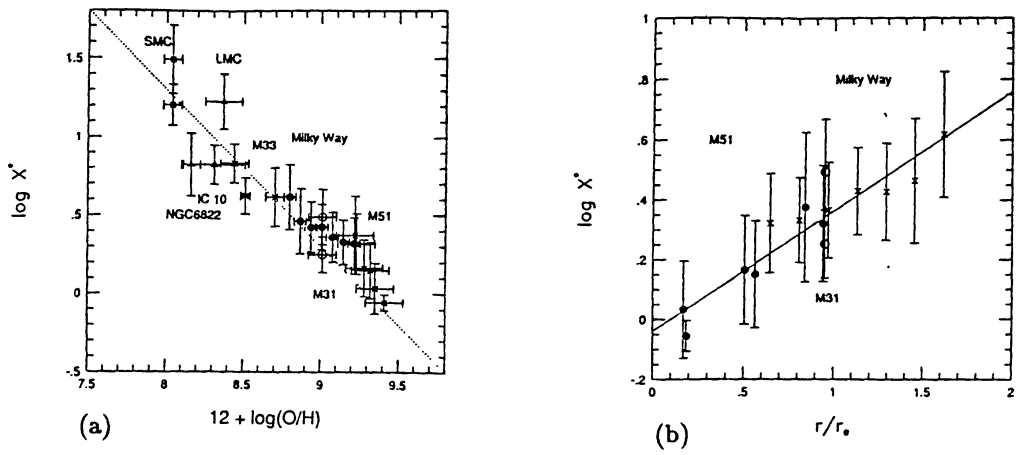

Figure 7. (a) Conversion factors for nearby galaxies against metallicity. (b) Conversion factor as a function of the distance from the galactic center.

ten adopt the empirical value obtained for molecular clouds in the Galaxy, $X \sim 2 - 3 \times 10^{20}$ (Bloemen et al. 1986).

The conversion factor varies by more than a factor of several between the Galactic Center and the outer arms and by more than an order of magnitude from normal spirals to metal-poor dwarfs like the Magellanic Clouds to the metal-rich galaxy M51 (Arimoto et al. 1996; Nakai & Kuno 1995). The conversion factor should be a complex function of interstellar conditions (metal abundance, density, temperature, and radiation fields). Arimoto et al. (1996) have examined the dependency of X on metallicity, as it is the best studied quantity among the others in external galaxies. They used X values derived by the virial-mass method. Fig. 7a shows conversion factors obtained in nearby galaxies against the O abundance, $12 + \log \mathrm{O/H}$. The diagram demonstrates that X is proportional to the metallicity and can be fit by $\log X^* = -1.0(12 + \log \mathrm{O/H}) + 9.30$. It is also known that O/H varies with absolute magnitude M_B of galaxies, $12 + \log \mathrm{O/H} = -0.20 M_B + 4.86$ (Roberts & Haynes 1994). We can then estimate a typical X value for a galaxy with known luminosity, $\log X^* = 0.20 M_B + 4.44$. This figure indicates that X is a simple function of metallicity in individual regions (clouds).

4.3. IMPLICATION OF THE CONVERSION FACTOR ON THE STUDY OF STAR FORMING EFFICIENCY AND DISK STABILITY

As the metallicity decreases with radius within a disk galaxy, the metallicity dependence of X implies a radial gradient in individual galaxies. In Fig. 7b we plot X^* as a function of radius r normalized by the effective radius r_e of the stellar disk for the galaxies, M51 and M31. The plot can be fit by $\log X^* = 0.37 + 0.40(r/r_e - 1)$. If we apply this radial gradient in deriving molecular hydrogen masses, we may expect a factor of two or three less

molecular gas in the central region than previously estimated. For example, Fig. 1 shows the CO intensity is proportional to the blue light intensity. If the conversion factor is smaller at the center, this means the SF efficiency is higher in the central region, which will also affect the current studies of star formation (e.g., Kennicut 1989).

The smaller gas mass in the central region would be crucial for the stability analysis of the nuclear gas disk. If the gaseous mass is by a factor of three or more smaller than that so far estimated, the nuclear gas disk will be no longer self-gravitating as often mentioned in theoretical models. This implies that the gas kinematics of the central regions of galaxies can be a good indicator of the stellar mass potential.

References

Arimoto, N., Sofue, Y., & Tsujimoto, T. 1996 A&A, submitted.
Bloemen, J. B. G. M. et al. 1986, A&A 154, 25
Bosma, A. 1981, AJ, 86, 1825.
Combes, F. 1991 ARAA, 29, 195.
Elmegreen, B. G. 1993, ApJ 411, 170.
Garcia-Burillo, S., Guélin, M., & Cernicharo, J. 1993, A&A, 274, 123.
Garcia-Burillo, S., Guélin, M., Cernicharo, & J., Dahlem, M. 1992, A&A, 266, 210.
Honma, M., Sofue, Y., & Arimoto, N. 1995 A&A 296, 33.
Ishizuki, S., Kawabe, R., Ishiguro, M., Okumura, S. K., Morita, K. -I., Chikada, Y., Kasuga, T., & Doi, M. 1990 ApJ 355, 436
Kennicutt, Jr . R. C. 1989 ApJ 344, 685.
Miyamoto, M., & Nagai, R. 1975, PASJ **27**, 533.
Morris, M., & Rickard, L.J. 1982, ARAA, 20, 517.
Nakai, N., & Kuno, N., 1995 PASJ, 47, 761.
Nakai, N., Kuno, N., Handa, T., & Sofue, Y. 1994, PASJ 46, 527.
Roberts, M. & Haynes, M. P. 1994, ARAA 32, 115.
Rots, A. H., Bosma, A., van der Hulst, J. M., Athanassoula, E., & Crane, P. C. 1990, AJ 100, 387.
Rubin, V. C., Ford, W. K., & Thonnard, N. 1982, ApJ, 261, 439
Rupen, M. P. 1991, AJ 102, 48.
Sargent, A. I., & Welch, W. J. 1993, ARAA 31, 297.
Scoville, N. Z., Thakker, D., Carlstrom, J. E., & Sargent, A. E. 1993 ApJ 404, L63.
Sofue, Y. 1996 ApJ 458, 120.
Sofue, Y., & Nakai, N. 1993, PASJ 45, 139
Sofue, Y., Honma, M., & Arimoto, N. 1994 A&A 296, 33.
Sofue, Y., Doi, M., Ishizuki, S., Nakai, N., & Handa, T. 1988 PASJ 40, 511.
Sofue, Y., & Nakai, N. 1993, PASJ 45, 139.
Young, J. S., & Scoville, N. 1982, ApJ 258, 467.
Young, J. S., & Scoville, N. Z. 1991, ARAA, 29, 581.
Wada, K., & Habe, A. 1996, MNRAS, in press.